Nanoscale Res Lett (2010) 5:786–790
DOI 10.1007/s11671-010-9559-4

NANO EXPRESS

A Nonaqueous Approach to the Preparation of Iron Phosphide Nanowires

Houde She · Yuanzhi Chen · Ruitao Wen · Kui Zhang · Guang-Hui Yue · Dong-Liang Peng

Received: 7 January 2010 / Accepted: 30 January 2010 / Published online: 16 February 2010

Abstract Previous preparation of iron phosphide nanowires usually employed toxic and unstable iron carbonyl compounds as precursor. In this study, we demonstrate that iron phosphide nanowires can be synthesized via a facile nonaqueous chemical route that utilizes a commonly available iron precursor, iron (III) acetylacetonate. In the synthesis, trioctylphosphine (TOP) and trioctylphosphine oxide (TOPO) have been used as surfactants, and oleylamine has been used as solvent. The crystalline structure and morphology of the as-synthesized products were characterized by powder X-ray diffraction (XRD) and transmission electron microscopy (TEM). The obtained iron phosphide nanowires have a typical width of $\sim$16 nm and a length of several hundred nanometers. Structural and compositional characterization reveals a hexagonal Fe_2P crystalline phase. The morphology of as-synthesized products is greatly influenced by the ratio of TOP/TOPO. The presence of TOPO has been found to be essential for the growth of high-quality iron phosphide nanowires. Magnetic measurements reveal ferromagnetic characteristics, and hysteresis behaviors below the blocking temperature have been observed.

Keywords Iron phosphides · Nanowire · Synthesis · Magnetic properties

H. She · Y. Chen (✉) · R. Wen · K. Zhang · G.-H. Yue · D.-L. Peng (✉)
Department of Materials Science and Engineering, College of Materials, Research Center for Materials Design & Application, Xiamen University, 361005 Xiamen, People's Republic of China
e-mail: yuanzhi@xmu.edu.cn

D.-L. Peng
e-mail: dlpeng@xmu.edu.cn

H. She
e-mail: shehoude@gmail.com

R. Wen
e-mail: compliment_care@xmu.edu.cn

K. Zhang
e-mail: zhang_ki@xmu.edu.cn

G.-H. Yue
e-mail: yuegh@xmu.edu.cn

Introduction

Nanoscale building blocks have attracted much interest due to their potential applications in replacement of traditional materials in the coming next few decades. However, most of the work in the synthesis of nanocrystals using solution-phase chemical method is focused on VI-II semiconductor systems and noble metals [1]. Transition metal phosphides exhibit unique catalytic, optical, electronic, and magnetic properties depending on their phases [2]. For example, Fe_3P is ferromagnet that has a high transition temperature ($T_c = 716$ K) [3], while FeP_2 is a small-bandgap semiconductor with a T_c of 15 K. Some preparation methods have been developed for the interest of studying the size-property relations of nanoscale iron phosphides. For example, Gu et al. [4] prepared 200 nm orthorhombic FeP via solvothermal synthesis employing $FeCl_3$ and Na_3P at 180°C. Luo et al. [5] synthesized nanocrystalline Fe_2P in a similar way at 180°C. Hu et al. [6] obtained a mixture of iron oxide nanoshells and hollow iron phosphide nanoparticles using sonichemistry method. Brock et al. [3] prepared FeP nanoparticles via a de-silylation route using a highly reactive phosphine source, $P(SiMe_3)_3$. Later, Brock [7] found that trioctylphosphine (TOP), which is a less-reactive reagent compared with $P(SiMe_3)_3$, can be used as phosphine source as well as surfactant and solvent in the

preparation of MnP and FeP using metal carbonyls as metal source. Liu et al. [8] synthesized FeP nanorods by injecting $Fe(CO)_5$/TOP into hot solution of TOP and trioctylphosphine oxide (TOPO). Hyeon et al. [9] studied the relation between the injection rate and length of Fe_2P nanorods synthesized using a syringe pump. Fe_2P nanorods can also be prepared without using a syringe pump as shown in the work of Whitmire et al. [10] who developed a single-source organometallic method to control morphology by varying the ratio of tri-*n*-octylamine (TOA) to oleic acid (OA) in a one-pot reaction.

We recently reported the synthesis of Ni_2P nanowires in the system of TOA/OA via an injection approach [11]. In this work, we present a primary result on the synthesis of iron phosphide nanowires using a solution-phase chemical approach. Instead of using toxic and unstable iron carbonyl compounds that were usually employed in most of previous work on the synthesis of iron phosphide nanowires, we developed a approach that uses a metal precursor of iron (III) acetylacetonate ($Fe(acac)_3$),which is low toxicity, inexpensive and rather stable at ambient condition. The structure and magnetic properties of as-synthesized nanowires are also presented in this work.

Experimental Section

Synthesis

In a typical synthesis, 0.5 mmol of $Fe(acac)_3$ (96%, Acros) was added in 10 mL of oleylamine (OM, 80–90%, Acros) and heated to 130°C. The resulting solution was continuously injected into a stock solution of 5 ml of OM, 5 mmol of TOP (97%, Acros), and 2.5 mmol of TOPO (90%, Acros) at 340°C using a syringe pump. The whole injection time varied from 3 to 6 h. A one-pot reaction was also attempted by reacting a mixture of 0.5 mmol of $Fe(acac)_3$, 4 mmol of TOP, 2 mmol of TOPO, and 6 mL of OM directly at 350°C for 1 h. The obtained product precipitates were washed by hexane and acetone, and separated from solution by centrifugation.

Characterization

Powder X-ray diffraction (XRD) data were collected on a Panalytical X'pert PRO X-ray diffractometer using Cu K_α radiation. Transmission electron microscopy (TEM) was performed on a TECNAI F-30 transmission electron microscope. Samples for TEM analyses were prepared by sonicating the as-synthesized powders in hexane and dropping a small volume onto a carbon-coated copper TEM grid followed by solvent evaporation. Magnetic analysis was performed using a superconducting quantum interference device (SQUID) magnetometer (MPMS-5).

Results and Discussion

Figure 1a shows the low-resolution TEM image of the iron phosphide wires prepared using injection method. The nanowires typically have a width of $\sim$16 nm and a length of several hundred nanometers. The selected area diffraction (SAED) pattern recorded from bundles of nanowires can be indexed to hexagonal Fe_2P. High-resolution TEM (HRTEM) images were taken on individual nanowires to observe their microstructures. As shown in Fig. 1b, the single nanowire exhibits single-crystalline characteristics. The measured lattice fringes (0.344 nm) that are perpendicular to the growth direction correspond well to the lattice spacing of (001) planes, indicating a growth direction of [001]. Park et al. [9] also reported a similar result for the growth direction of Fe_2P nanowires. Typical XRD pattern of the as-prepared iron phosphide samples is shown in Fig. 1c. The observed diffraction peaks also can be indexed with hexagonal Fe_2P structure, agreeing well with the SAED analytic result. Energy-dispersive X-ray spectroscopy (EDS) analysis on individual nanowires (Fig. 1d) reveals Fe and P peaks, confirming the formation of iron phosphide. Further quantitative analysis reveals a Fe: P ratio of $\sim$1.93:1, which is close to the stoichiometric ratio of Fe_2P.

It can be inferred from the above results that the anisotropic shape of nanowires comes mainly from the intrinsically anisotropic nature of hexagonal crystalline structure. The monomer concentration of the injection route is relatively low, which favors the growth of existing seeds formed in the early stage of continuous delivery. Another important prerequisite for the formation of anisotropic nanostructures is related to the surfactants used. Usually, a multi-surfactant system favors the formation of an anisotropic nanostructure. In our case, the employed TOP and TOPO both can act as surfactants to cover different crystallographic surfaces of newly formed nanocrystal seeds, and eventually lead to the anisotropic growth toward c axis, forming a one-dimensional nanostructure.

The formation of iron phosphide is closely related to the reaction temperature. Our studies found that if the experiments were conducted below 320°C, the as-synthesized products were mainly iron oxide nanoparticles, which indicates that necessary thermal energy is needed to decompose TOP to form active phosphorus atoms to take part in the phosphide formation. TOP concentration is also an important factor that influences the synthesized products. For example, iron nanoparticles were obtained when TOP concentration was relatively low (less than 2 mmol).

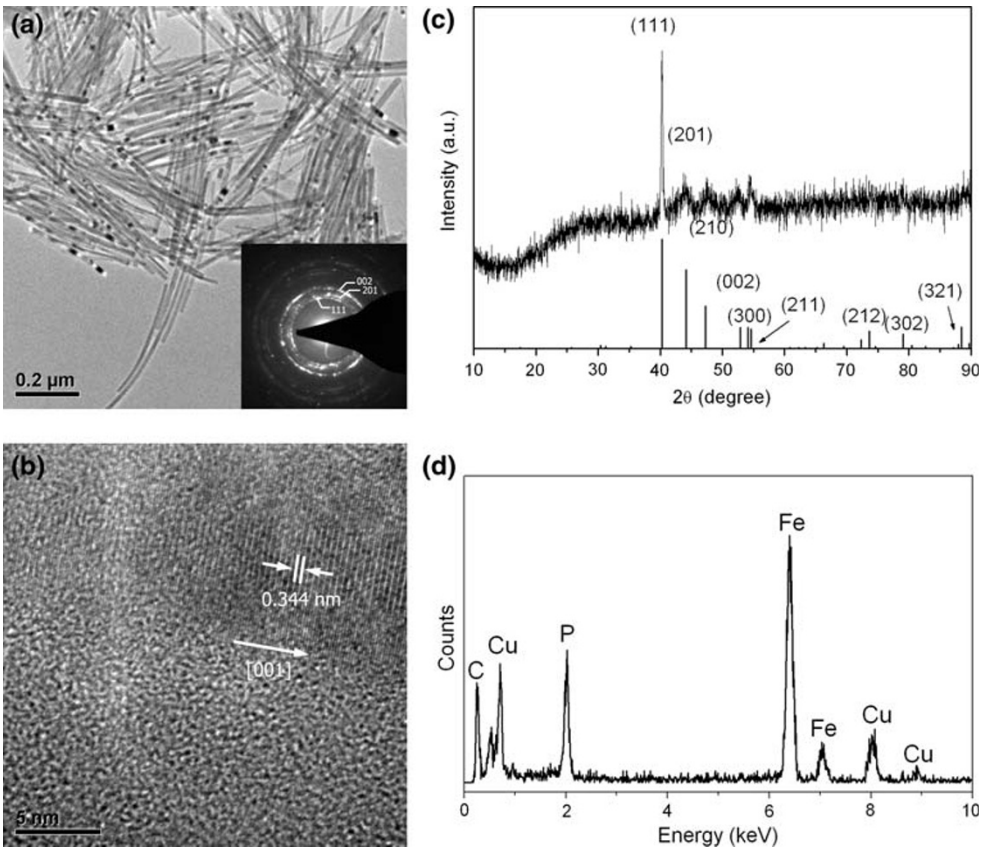

Fig. 1 Normal TEM image along with SAED pattern (**a**), HRTEM image (**b**), XRD pattern (**c**) and EDS spectrum (**d**) of the as-prepared iron phosphide nanowires

However, when high concentration of TOP (e.g. 12 mmol) was used, the synthesized nanowires would have a curved morphology (see Fig. 2a), reflecting the insufficient capability of TOP for the protection of nanowires' sidewalls. A small variation of TOP amount (from 3 to 5 mmol) did not make apparent difference in the products, showing the robustness of our synthetic approach. The employed surfactant TOPO also plays an important role in controlling the product's morphology. If no TOPO is added, the synthesized products mainly exhibit a nanoblock-like morphology resulting from the agglomeration of many soft-warped nanowires. This indicates that the existence of TOPO may function as a sidewall protector that can keep iron phosphide nanowires grow straightly over hundreds of nanometers. However, high concentration of TOPO on the contrary will reduce the quality of nanowires and lead to the formation of some big nanoblocks in the products.

The formation process of Fe_2P nanowires may be as follows. At first, the complex of $Fe(acac)_3$-OM decomposes to iron clusters once added to hot solvent of OM. Then, these iron clusters will be attached to TOP molecules, and the P–C bonds located at the particle surface may break and cause phosphorus to react with iron, forming iron phosphide. Once Fe_2P seeds with an anisotropic structure forms, the growth along [001] direction will be favored due to the cooperation of anisotropic nature and the side-protection effect of surfactant molecules. This eventually leads to the formation of a one-dimensional nanostructure.

We also explored one-pot reaction for the synthesis of iron phosphide nanowires. As shown in Fig. 2b, the obtained products via one-pot reaction consist of nanowires plus nanosheets or nanoblocks. The shape singularity of the products from the one-pot reaction is not superior to the continuous-injection approach. Considering the robustness of the reaction, this difference should not come from the small difference in TOP amount. It is certain that continuous-injection route is crucial to keep the singularity of the products. A possible reason is that one-pot synthesis incurs a high concentration of nuclei, some of which are unable to develop into nanowires due to insufficient protections of surfactant molecules, whereas for the injection approach, the nuclei concentration at the beginning stage is restricted by the delivering rate, and the relatively low concentration of nuclei plus the continuous delivery of source materials will allow nuclei to fully grow into nanowires.

The hysteresis loop of as-prepared Fe_2P nanowires measured at 5 K is shown in Fig. 3a. It is clear that the magnetization curve is difficult to be saturated and the unsaturated magnetization moment is 45.5 emu/g (1.16 μ_B), which is much lower than the saturation magnetization (M_s) value of bulk Fe_2P (2.81 μ_B) [12]. Meanwhile, the

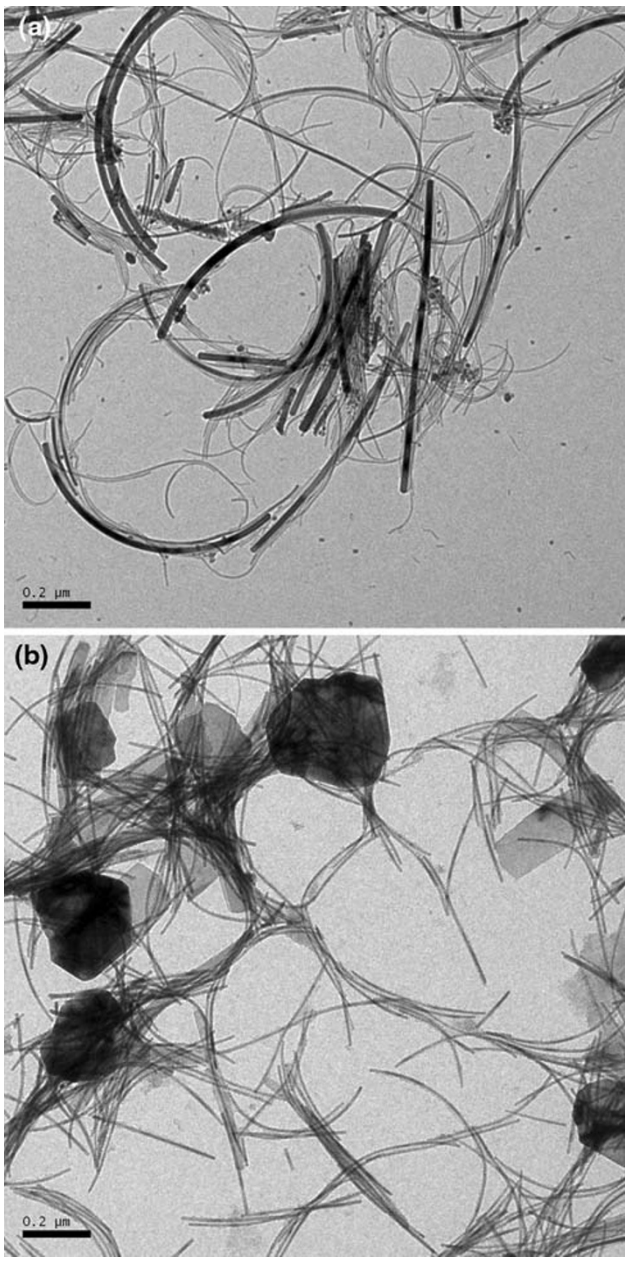

Fig. 2 TEM images of iron phosphide nanowires with a curved morphology synthesized using high concentration of TOP (**a**), and products synthesized using one-pot reaction (**b**)

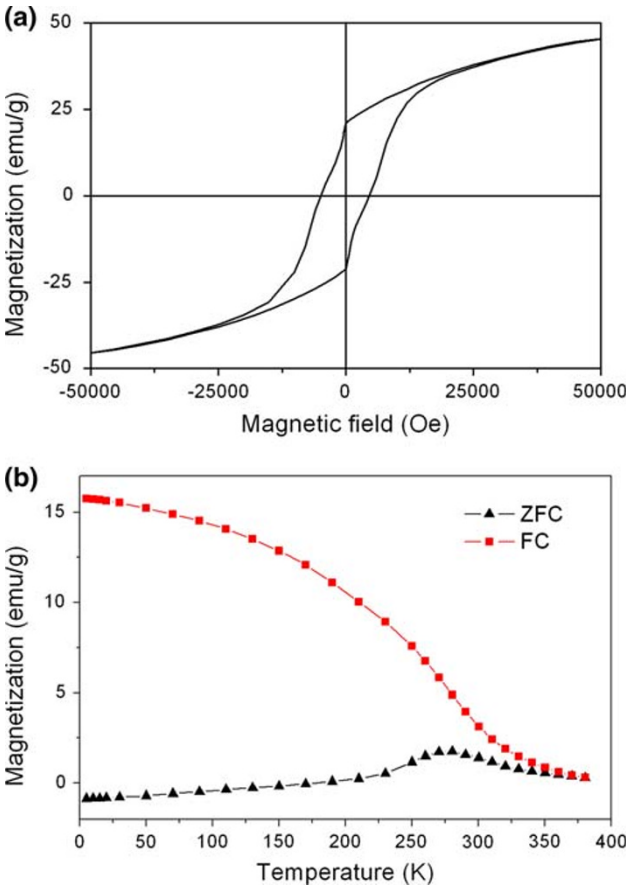

Fig. 3 **a** Hysteresis loop measured at 5 K and **b** ZFC/FC curves at an applied field of 100 Oe for the as-prepared iron phosphide nanowires

measured coercive force is about 5,000 Oe. A large coercive force has also been noticed in Fe_2P nanorod ($H_c = 3.9$ kOe) [13] and nanoparticle samples ($\sim$5 kOe) [5]. From the curve of Fig. 3a, we can see that this curve is not very smooth. In fact, it looks like that the curve is a result of combination of two different loops. Such a slightly twisted loop indicates that a small amount of impurities may exist in the synthesized products, although their amounts may beyond the detection limit of XRD. Since SQUID is a characterization technology that is very sensitive to a trace amount of magnetic impurities, it can detect these impurities more easily. It is very likely that a small amount of Fe or Fe oxides constitute the impurities, since they were often found in the experiments performed at lower temperatures. Such impurities were considered as the main reason accounting for the twisted hysteresis loops of Fe_2P nanorods [10]. Similar results have also been observed in FePt nanoparticle samples, which also have a large coercivity [14]. Figure 3b shows the zero-field-cooled (ZFC) and field-cooled (FC) curves of Fe_2P nanowires measured in a temperature range of 5–300 K. A high blocking temperature ($\sim$275 K) is observed, which is consistent with the hysteresis test at 300 K (not included in this paper).

Conclusions

Iron phosphide nanowires have been synthesized through a nonaqueous approach that utilizes $Fe(acac)_3$ as an iron source, TOP as a phosphorus source and oleylamine as solvent. The as-prepared nanowires have a hexagonal Fe_2P structure and grow along c axis. The dimension of nanowires can be tuned via reaction parameters such as

injection rate, reaction temperature, and TOP/TOPO ratio. Both injection method and one-pot reaction can produce iron phosphide nanowires, although the former can generate products with much better uniformity and yield. The magnetic tests reveal ferromagnetic characteristics below the blocking temperature, and a large coercive force of $\sim$5,000 Oe has been observed. The reported synthetic approach does not use commonly used toxic iron carbonyl compounds as iron precursor, which provides a convenient access to further studies of their special physical and chemical properties.

Acknowledgments This work was partially supported by the National Natural Science Foundation of China (Grant nos. 50701036 and 50671087) and the National Outstanding Youth Science Foundation of China (Grant no. 50825101).

References

1. T. Hyeon, S.S. Lee, J. Park, Y. Chung, H.B. Na, J. Am. Chem. Soc. **123**, 12798 (2001)
2. S.L. Brock, K. Senevirathne, J. Solid State Chem **181**, 1552 (2008)
3. S.C. Perera, P.S. Fodor, G.M. Tsoi, L.E. Wenger, S.L. Brock, Chem. Mater **15**, 4034 (2003)
4. Y. Gu, G. Fan, Y. Qian, H. Zheng, Z. Yang, Mater. Res. Bull **37**, 1101 (2002)
5. F. Luo, H.-L. Su, W. Song, Z.-M. Wang, Z.-G. Yan, C.-H. Yan, J. Mater. Chem **14**, 111 (2004)
6. C.G. Hu, Y. Li, J.P. Liu, Y.Y. Zhang, G. Bao, B. Buchine, Z.L. Wang, Chem. Phys. Lett. **428**, 343 (2006)
7. S.L. Brock, S.C. Perera, K.L. Stamm, Chem. Eur. J **10**, 3364 (2004)
8. C. Qian, F. Kim, L. Ma, F. Tsui, P. Yang, J. Liu, J. Am. Chem. Soc. **126**, 1195 (2004)
9. J. Park, B. Koo, Y. Hwang, C. Bae, K. An, J.G. Park, H.M. Park, T. Hyeon, Angew. Chem. Int. Ed. Eng **43**, 2282 (2004)
10. A.T. Kelly, I. Rusakova, T. Ould-Ely, C. Hofmann, A. Luttge, K.H. Whitmire, Nano Lett **7**, 2920 (2007)
11. Y. Chen, H. She, X. Luo, G.-H. Yue, D.-L. Peng, J. Cryst. Growth **311**, 1229 (2009)
12. A. Koumina, M. Bacmann, D. Fruchart, J.L. Soubeyroux, P. Wolfers, J. Tobola, S. Kaprzyk, S. Niziol, M. Mesnaoui, R. Zach, Ann. Chimie Sci. Materiaux **23**, 177 (1998)
13. J. Park, B. Koo, K.Y. Yoon, Y. Hwang, M. Kang, J.-G. Park, T. Hyeon, J. Am. Chem. Soc. **127**, 8433 (2005)
14. T. Iwaki, Y. Kakihara, T. Toda, M. Abdullah, K. Okuyama, J. Appl. Phys **94**, 6807 (2003)